NINTH EUROPEAN ROTORCRAFT FORUM

Paper No. 54

AEROMECHANICAL STABILITY OF A HINGELESS ROTOR IN HOVER AND FORWARD FLIGHT: ANALYSIS AND WIND TUNNEL TESTS

WILLIAM T. YEAGER, JR.

NASA/Langley Research Center
Army Structures Laboratory
Hampton, Virginia
U.S.A.

M-NABIL H. HAMOUDA

Vigyan Research Associates, Inc.
Hampton, Virginia
U.S.A.

WAYNE R. MANTAY

NASA/Langley Research Center
Army Structures Laboratory
Hampton, Virginia
U.S.A.

September 13-15, 1983

STRESA, ITALY

Associazione Industrie Aerospaziali

Associazione Italiana di Aeronautica ed Astronautica

AEROMECHANICAL STABILITY OF A HINGELESS ROTOR IN HOVER AND FORWARD FLIGHT: ANALYSIS AND WIND TUNNEL TESTS

ABSTRACT

A research effort of analysis and testing has been conducted in the NASA-Langley Transonic Dynamics Tunnel to investigate the ground resonance phenomenon of a soft in-plane hingeless rotor. Experimental data were obtained using a 9 ft. (2.74 m) diameter model rotor in hover and forward flight. Eight model rotor configurations were investigated. Configuration parameters included pitch-flap coupling, blade sweep and droop, and precone of the blade feathering axis. An analysis based on a comprehensive analytical model of rotorcraft aerodynamics and dynamics was used for this study. The moving-block method was used to experimentally determine the regressing lead-lag mode damping. Good agreement has been obtained between the analysis and test. Both analysis and experiment indicated ground resonance instability in hover. The paper presents an outline of the analysis, a description of the experimental model and procedures, and comparison of the analytical and experimental data.

1.0 Introduction

Aeromechanical stability problems which involve interaction of the rotor and airframe are usually divided into the categories of ground and air resonance. While the terminology may imply totally different phenomena, both are self-excited instabilities caused by the coupling between blade lagging motion and hub motion in the plane of the rotor [1-3]. Although aeromechanical instability is traditionally associated with articulated rotors, hingeless rotors are also susceptible to this problem. Hingeless rotors are classified into two types. One is associated with a soft inplane system having the blade inplane frequency less than the rotor rotational speed, and the other with a stiff inplane system where the blade inplane frequency is higher than the rotor rotational speed. This paper deals specifically with ground resonance of soft inplane hingeless rotors.

Ground resonance can occur with helicopter rotor models just as it can occur with full scale helicopters. The resonance is characterized by a coalescence of the blade lead-lag regressing frequency (less than the rotor speed) with a body vibration mode. For a full scale helicopter, the body softness is usually related to a landing gear associated frequency when the vehicle is in contact with the ground. For wind-tunnel helicopter models, the body mode frequency usually results from the model being attached to either a mounting strut or a flexible force balance. Ground resonance is now a

well understood phenomenon [4], particularly for articulated rotors. However, hingeless rotors provide substantial structural and aerodynamic couplings that complicate their aeromechanical stability problems. A number of analytical models [5-7] have been developed to investigate the aeromechanical stability of hingeless rotors. However, these analytical models have a number of limitations as indicated in Reference 8. Correlations between theory and experiment have also been made [9-11]. These comparisons have been limited to hover and the use of small-scale models in forward flight.

To investigate the ground resonance of soft inplane hingeless rotors, an analytical and experimental study was conducted in the NASA Langley Transonic Dynamics Tunnel. This effort was intended to aid in the identification of an analysis that can be used in both the design and testing phases of hingeless and bearingless rotor development. Another objective of the research was to develop an experimental technique for blade excitation and damping measurements in the rotating system.

The paper presents an outline of the analytical model and describes the experimental model and procedures. Correlations between the theory and experiment in both hover and forward flight are presented. Finally, the effects of rotor coupling parameters on the stability characteristics are discussed. These parameters are blade sweep and droop, precone of the blade feathering axis and pitch-flap coupling.

2.0 Analytical Model

The Comprehensive Analytical Model of Rotorcraft Aerodynamics and Dynamics (CAMRAD) computer program was used as the theoretical tool for this investigation. The code was developed by Johnson [12, 13]. The solution for the system aeroelastic stability proceeds as follows: 1) the data input, 2) the trim solution, and 3) the flutter analysis.

The structural dynamic model of the rotor input to CAMRAD includes elastic degrees of freedom in flap bending, lead-lag bending and torsion, plus a rigid pitch degree of freedom. The blade is represented by a spanwise distribution of mass, bending and torsion stiffness and moment of inertia. An estimate of structural damping has also been included in the rotor data. The aircraft model consists of elastic motion of the fuselage and rotor support system in the wind tunnel. The airframe data input includes generalized mass, structural damping, frequency and mode shape of the elastic modes. These modal characteristics are set to the measured values. The rotor blade aerodynamic forces are calculated using lifting line theory and steady two-dimensional airfoil characteristics

with corrections for unsteady and three-dimensional flow effects. The rotor non-uniform inflow is calculated using a vortex-wake model. The airfoil characteristics are constructed using analytical expressions [13]. Fuselage aerodynamic loads are neglected. The degrees of freedom used in the stability analysis are the flap and lag motion of the blades, the body pitch and roll motions and rotor dynamic inflow.

In the trim analysis the controls are iterated until the required operating state is achieved. The trim analysis is performed first for uniform inflow, then for nonuniform inflow with a prescribed wake, and finally for nonuniform inflow with a free wake geometry.

In the flutter analysis, the dynamics of the system is described by a set of linear differential equations. These equations represent the perturbed motion of the helicopter from the trim condition. The stability of the system is determined in terms of the eigenvalues and eigenvectors of the constant coefficient (in hover) or periodic coefficient (in forward flight) equations.

3.0 Experimental Models and Procedures

3.1 Model Description

The rotor model used for this investigation is a soft in-plane hingeless rotor. The principal rotor properties are listed in Table 1. The rotor system is not a dynamically scaled representation of a specific aircraft but rather is representative of a typical full-scale aircraft design based on Mach number, mass ratio and frequency simulation. The model blades were fabricated with fiberglass spars specifically for

Table 1. Principal Rotor Properties

Parameter	Value
Rotor Type	Research Hingeless Hub
Number of Blades	4
Rotor Diameter	9 ft. (2.74 m)
Blade Chord	4.24 in. (1.67 cm)
Solidity	0.10
Airfoil Section	NACA 0012
Blade Twist	0 Degrees
Blade Elastic Axis	25% Chord
Blade Pitch Axis	25% Chord
Center of Gravity	25% Chord

testing in the Freon-12[1] test medium of the Langley Transonic Dynamics Tunnel.

The rotor hub, shown in Figure 1, consists of metal flexures to accommodate flap and lead-lag motions and a mechanical feathering hinge to allow blade pitch motion. The flap and lead-lag flexures are each strain-gaged and calibrated to measure motion in those directions. The hingeless hub has the capability to independently vary blade sweep, droop, and precone of the blade feathering axis. These changes are accomplished by means of angle blocks as shown in Figure 2. Two values of blade pitch-flap coupling are also available. A list of rotor configurations tested is given in Table 2.

Table 2. Rotor Configuration Parametric Values

Configuration	δ_3 (a) (deg)	Sweep (b) (deg)	Droop (c) (deg)	Pre-cone (d) (deg)
Baseline	0	0	0	0
1	42.5	0	0	0
2	0	+2	0	0
3	0	0	+2	0
4	42.5	0	+4	+3
5	42.5	0	+2	+3
6	42.5	0	-2	+3
7	42.5	0	+4	+6

a - pitch-flap coupling angle
b - positive aft
c - positive down
d - positive up

The test-bed used for the experiment is the Langley Aeroelastic Rotor Experimental System (ARES). The ARES, shown in Figure 3, consists of a rotor drive system and rotor control system enclosed by a streamlined helicopter fuselage shape. The ARES is mounted on a six-component strain-gage balance which is fixed with respect to the rotor shaft and thus pitches with the ARES. Fuselage forces and moments are not sensed by the balance. The entire ARES and balance assembly are mounted on a rigid stand bolted to the floor of the wind tunnel. The ARES rotor control system and fuselage pitch attitude are

[1]Freon-12 is a registered trademark of E.I. duPont de Nemours and Co., Inc.

remotely controlled from within the wind-tunnel control room. The swashplate is moved by three hydraulic actuators. Instrumentation on the ARES and in the wind-tunnel control room allows continuous displays of model control settings, rotor forces and moments, blade loads, and pitch link loads. ARES pitch attitude is measured by an accelerometer, and rotor control positions are measured by linear potentiometers connected to the swashplate. Rotating system data are transferred into the fixed system through a 30-channel slipring assembly.

3.2 Wind Tunnel

The test was conducted in the Langley Transonic Dynamics Tunnel. This tunnel is a continuous flow tunnel with a slotted test section. The tunnel test section is 16 ft. (4.88 m) square with cropped corners and has a cross-sectional area of 248 ft^2 (23.04 m^2). Either air or Freon-12 may be used as a test medium. For this study, Freon-12 at a nominal density of 0.0047 slugs/ft^3 (2.42 Kg/m^3) was used as the test medium. Because of its high density and low speed of sound, the use of Freon-12 aids the matching of model-rotor-scale Reynolds number and Mach number to full-scale values. The heavier test medium permits a simplified structural design to obtain the required stiffness characteristics for dynamic similarity, and thus eases design and fabrication requirements of the model (ref. 14).

3.3 Test Procedures

Pre-wind-tunnel tests were conducted to determine the rotor blade frequencies as well as the ARES body modes and damping. A shake test was conducted to determine the non-rotating rotor blade natural frequencies. This information was desired to substantiate calculated values. Good agreement was obtained between measured frequencies and those predicted by the CAMRAD code. The first flap and lead-lag mode frequencies were predicted within 0.3 Hz. The rotor blade rotating natural frequency in the lead-lag direction was measured during the wind-tunnel test as will be discussed later. The calculated rotor first lead-lag and flap frequencies are 0.55/REV and 1.14/REV respectively for a nominal rotor speed of 618 rpm. The measured frequency and damping values of the ARES as mounted in the tunnel are given in Table 3. These data were input for the aeroelastic stability analysis.

Table 3. Measured ARES Dynamic Properties

Mode	Frequency Hz.	Damping % Critical
Roll	5.4	7.3
Pitch	5.9	5.7

Testing in hover was conducted for Configuration 1 over a range of rotor speeds from 400 rpm up to a value where rotor in-plane instability was encountered. All configurations shown in Table 2 were tested in forward flight at a rotor speed of 618 rpm. Advance ratio was varied up to 0.3 with three values of collective pitch set at each advance ratio.

At each test point the tunnel speed was adjusted to give the desired advance ratio. The model was then pitched to the desired shaft angle of attack and collective pitch was set. At each advance ratio, data were taken at shaft angles of attack of 0, -5, and -10 degrees. The corresponding collective pitch at each shaft angle of attack was 4, 8, and 12 degrees. Cyclic pitch control was used to remove the rotor first harmonic flapping with respect to the shaft. Once the test condition was established, a test technique was initiated to determine the inherent stability levels for the model. This test technique involved using the moving-block method described in Reference 15 as an interactive program to determine the rotor in-plane frequency and damping.

The test technique consisted of two steps. First, the model was excited in the fixed system by applying a longitudinal cyclic oscillation to the rotor through the swashplate. The amplitude of the swashplate oscillation was nominally 0.75 degrees. The frequency of the swashplate oscillation was initially set equal to the fixed system value of the rotor in-plane frequency (lead-lag regressing mode) predicted by CAMRAD. The swashplate oscillation was then adjusted slightly to obtain the maximum rotor in-plane response. Once the rotor in-plane response was established, the swashplate oscillation was removed and the moving-block procedure was initiated. A typical real-time moving-block display is shown in Figure 4. Utilization of this display was as described in reference 15. The frequency of interest was selected from the fast Fourier transform (FFT) of the lead-lag signal trace, and the damping ratio was computed from the log of the amplitude of the filtered lead-lag response. It is worth noting that in case of a ground resonance instability, not only was the swashplate excitation removed but the rotor speed was immediately reduced.

This action was sufficient to eliminate the rotor disturbance in the unstable region. By applying the moving-block technique, the rotor in-plane damping was measured in the rotating system. These damping values were then transferred into the fixed system as follows:

$$\zeta_F = \zeta_R \left(\frac{\omega_\zeta}{\Omega - \omega_\zeta}\right)$$

where:

ζ_F = fixed system damping ratio

ζ_R = rotating system damping ratio determined by the moving-block method

ω_ζ = rotating system first lead-lag mode regressing frequency determined by the moving-block method

Ω = rotor rotational speed

4.0 Results and Discussion

4.1 Hover

Testing in hover was conducted at 8 degrees collective pitch over a range of rotor speed from 400 rpm to a value where inplane instability was encountered. The predicted and measured stability of Configuration 1 versus rotor speed is shown in Figure 5. Figure 5(a) shows a predicted coalescence of the body roll mode frequency with the regressing lag mode frequency above 650 rpm. The predicted and experimental lead-lag frequency are seen to be in good agreement. Over the range of rpm tested, differences between the predicted and experimental values of lead-lag frequency average 0.3 Hz. As can be seen from Figure 5(b), the regressing lag mode damping in the fixed system is also well predicted. In the critical region near the indicated ground resonance instability, differences between the analytical and experimental damping ratio average 0.006. Inplane damping ratio decreases gradually until a sudden decrease occurs around 640 rpm. An unstable region is indicated near the regressing lag-roll resonance rotor speed. The predicted damping level has recovered to a positive value (stable) at 775 rpm. Due to rotor stress level limitations, the test could not be carried out for rotor speeds higher than 650 rpm. It is concluded that the analytical model accurately predicts ground resonance of hingeless rotors in hover.

Furthermore, the excitation technique using the swashplate actuators produces excellent stability data.

4.2 Forward Flight

Figure 6 shows the variation of the predicted and measured lead-lag mode damping with collective pitch for the baseline configuration at advance ratio = 0.2, 0.25 and 0.3. The rotor speed is 618 rpm. Both data and theory show a trend of generally increasing damping with collective pitch. The increased blade pitch angle generates aerodynamic and inertial flap-lag coupling that increases the lead-lag damping. A comparison of the damping levels for different advance ratios at constant collective pitch indicates that both the analysis and test show the lead-lag mode generally becomes more stable as the forward speed increases. Good correlation is shown between the analytical prediction of the damping and experimental data. It should be noted that for both the baseline configuration and all subsequent configurations discussed, differences between the analytical and experimental damping ratio average 0.004.

Results for Configuration 1 (δ_3 = +42.5°) are shown in Figure 7 for the regressing lead-lag damping versus collective pitch in forward flight at normal rotor speed (618 rpm). The agreement between the predicted and measured damping is good. Compared to the baseline configuration (no pitch-flap coupling) in Figure 6 it can be seen that there is a decrease in damping due to negative pitch-flap coupling (positive δ_3). This may be due to changes in pitch-lag stability caused by δ_3 as described in Reference 16.

Figure 8 shows the variation of predicted and measured lead-lag damping with collective pitch for Configuration 2 (2° aft blade sweep) in forward flight. As can be seen there is a good agreement between the analysis and test. Compared to the baseline zero sweep configuration in Figure 6, these data show that there is a change in damping with aft sweep.

The results for Configurations 3 and 4 are shown in Figures 9 and 10, respectively. These two configurations incorporate changes in blade droop and pre-cone. The predicted and measured lead-lag damping are seen to be in good agreement for both configurations. Similar correlations were obtained between the analysis and test for configurations 5, 6 and 7.

Presented in Figures 11 and 12 are the analytical and experimental lead-lag damping results which show the effect of two configuration parameters, namely blade droop and pre-cone angles on the damping levels. Figure 11 shows the variation of damping with collective pitch for three values of droop angle

in forward flight. For constant collective pitch, the lead-lag damping increases for decreasing droop angles. Figure 12 shows damping results for two different pre-cone angles. As can be seen, the configuration with a 6 degree positive pre-cone has higher lead-lag damping than the 3 degree positive pre-cone configuration.

5.0 Conclusions

Theoretical and experimental results for the aeromechanical stability of a soft-inplane hingeless rotor in hover and forward flight have been presented. The effect on rotor stability of pitch-flap coupling, blade sweep, droop, and pre-cone of the feathering axis has been demonstrated. Based on the results of this research the following conclusions have been reached:

1) Consistent and repeatable measurements of the rotor lead-lag regressing mode damping were made.

2) The analysis accurately predicted the ground resonance instability found by experiment in hover.

3) Good agreement was found between the theoretical and experimental frequency and damping values for the rotor lead-lag regressing mode in hover and forward flight. The theory predicted the correct trends with collective pitch, advance ratio, pre-cone, blade droop, and pitch-flap coupling.

6.0 References

1. Hohenemser, K. H.: Hingeless Rotorcraft Flight Dynamics. AGARD-AG-197, Sept. 1974.

2. Donham, R. E.; Cardinale, S. V.; and Sachs, I. B.: Ground and Air Resonance Characteristics of a Soft Inplane Rigid Rotor System. Journal of the American Helicopter Society, Vol. 14, No. 4, Oct. 1969, pp. 33-41.

3. Miao, Wen-Liu; and Huber, Helmut B.: Rotor Aeroelastic Stability Coupled with Helicopter Body Motion. NASA SP-352, Feb. 1974, pp. 137-146.

4. Coleman, R. P.; and Feingold, A. M.: Theory of Self-Excited Mechanical Oscillations of Helicopter Rotors with Hinged Blades. NACA Report 1351, 1958.

5. Young, Maurice I.; and Bailey, David J.: Stability and Control of Hingeless Rotor Helicopter Ground Resonance. Journal of Aircraft, Vol. 11, No. 6, June 1974, pp. 333-339.

6. Ormiston, Robert A.: Aeromechanical Stability of Soft Inplane Hingeless Rotor Helicopters. Presented at the Third European Rotorcraft and Powered Lift Aircraft Forum, Aix-en-Provence, France, Sept. 1977.

7. Hodges, D. H.: A Theoretical Technique for Analyzing Aeroelastic Stability of Bearingless Rotors. Proceedings of the 19th AIAA Structures, Structural Dynamics and Materials Conference, April 3-5, 1978, pp. 282-294.

8. Johnson, W.: Comprehensive Helicopter Analyses - A State of the Art Review. NASA TM-78539, 1979.

9. Burkam, John E.; and Miao, Wen-Liu: Exploration of Aeroelastic Stability Boundaries with a Soft-Inplane Hingeless Rotor Model. Journal of the American Helicopter Society, Vol. 17, No. 4, Oct. 1972, pp. 27-35.

10. Bousman, William G.: An Experimental Investigation of Hingeless Helicopter Rotor-Body Stability in Hover. NASA TM-78489, June 1978.

11. Weller, William H.: Correlating Measured and Predicted Inplane Stability Characteristics for an Advanced Bearingless Rotor. NASA CR-166280, Jan. 1982.

12. Johnson, W.: A Comprehensive Analytical Model of Rotorcraft Aerodynamics and Dynamics, Part I - Analysis Development. NASA TM-81182, 1980.

13. Johnson, W.: A Comprehensive Analytical Model of Rotorcraft Aerodynamics and Dynamics, Part II - User's Manual. NASA TM-81183, 1980.

14. Lee, Charles: Weight Considerations in Dynamically Similar Model Rotor Design. S.A.W.E. Paper No. 659, May 1968.

15. Hammond, C. E.; and Doggett, R. V., Jr.: Determination of Subcritical Damping by Moving-Block/Randomdec Applications. NASA SP-415, 1976.

16. Gaffey, Troy M.: The Effect of Positive Pitch-Flap Coupling (Negative δ_3) on Rotor Blade Motion Stability and Flapping, Journal of the American Helicopter Society, Vol. 14, No. 2, April 1969, pp. 49-67.

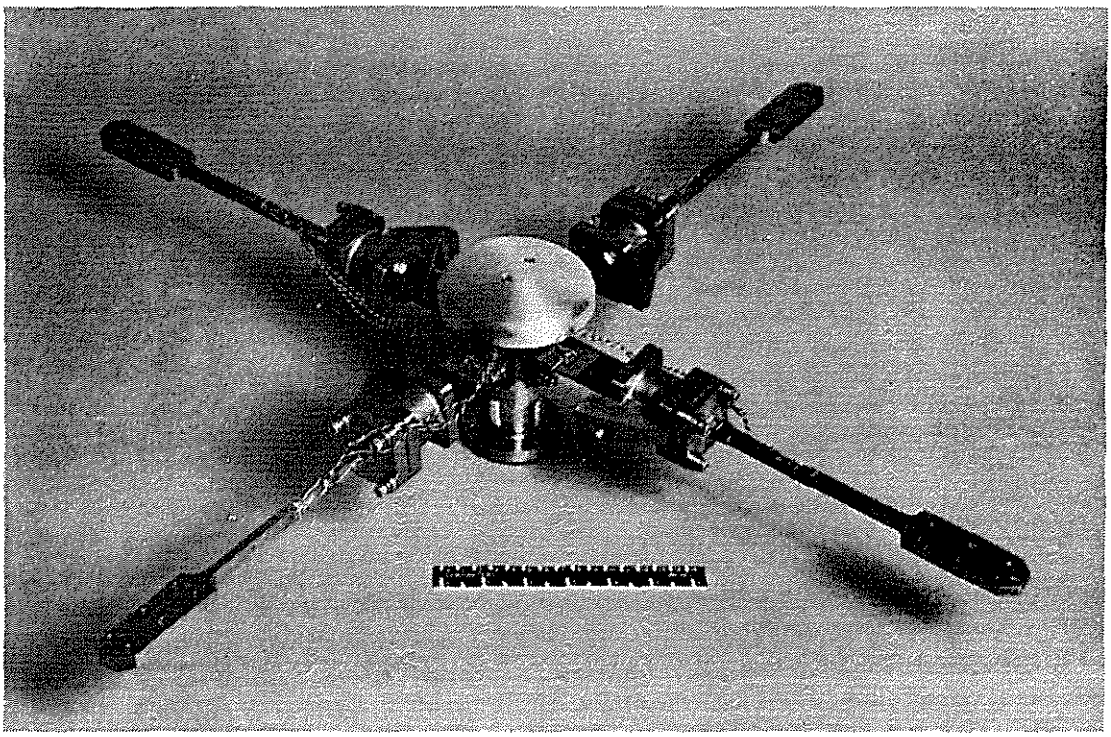

Figure 1. Model rotor hub.

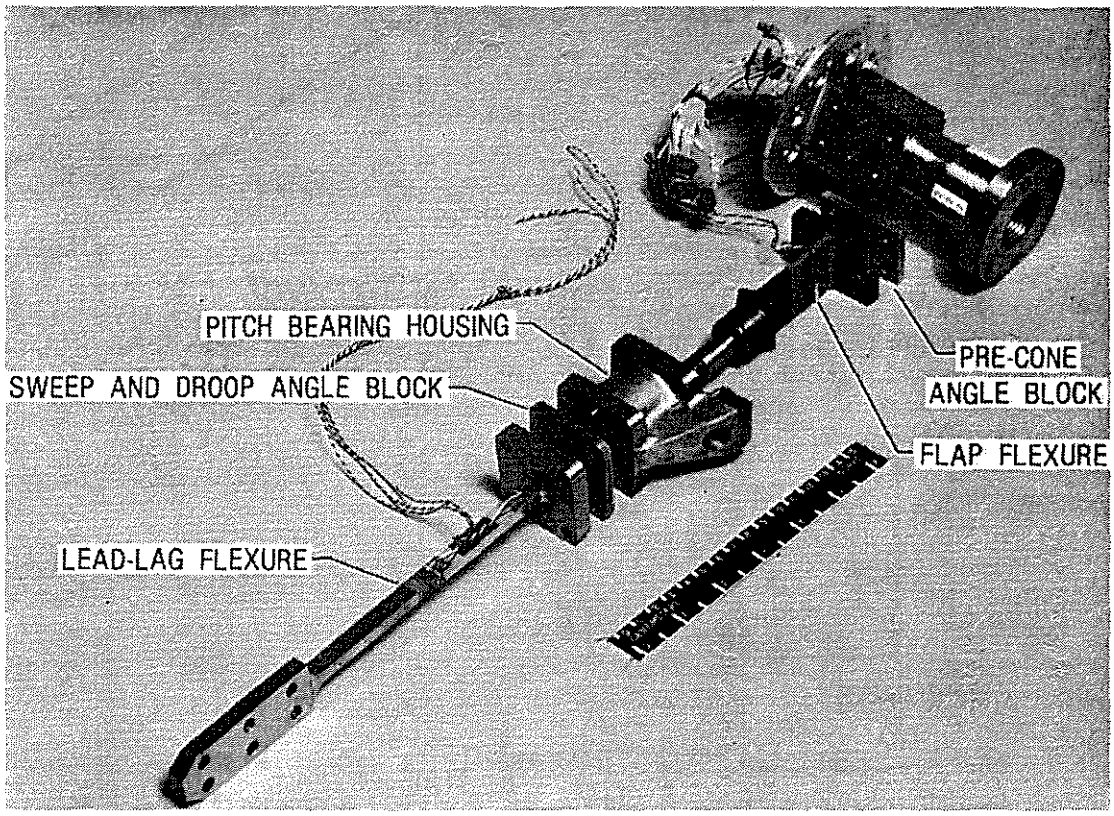

Figure 2. Details of rotor hub root flexures.

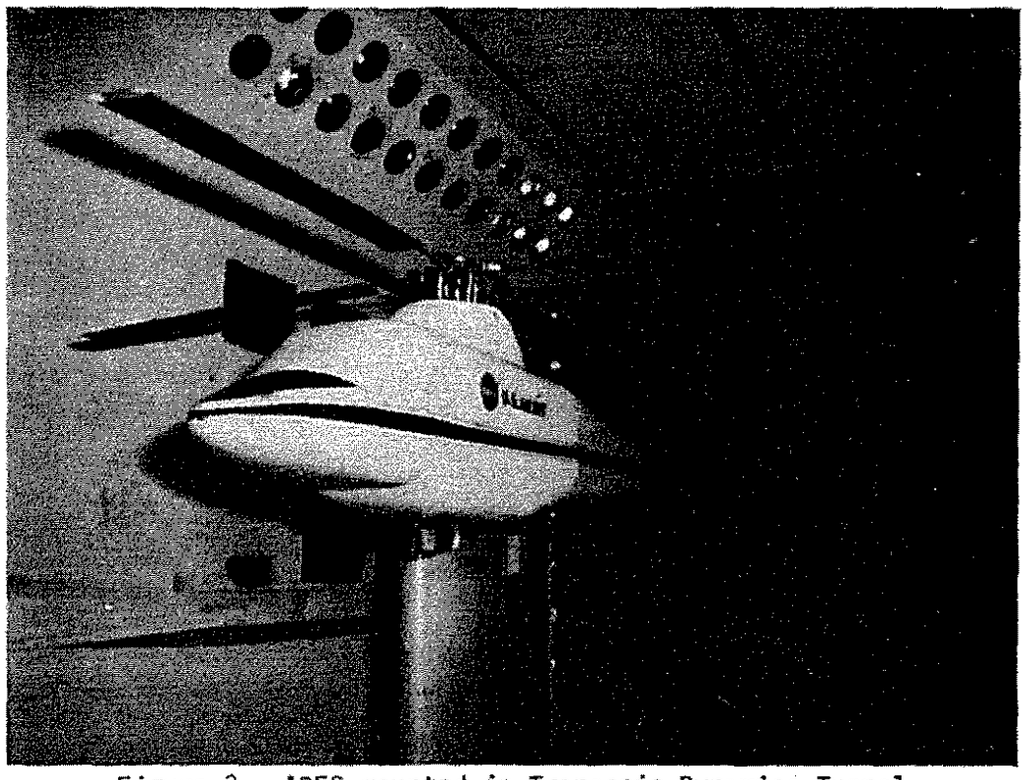

Figure 3. ARES mounted in Transonic Dynamics Tunnel.

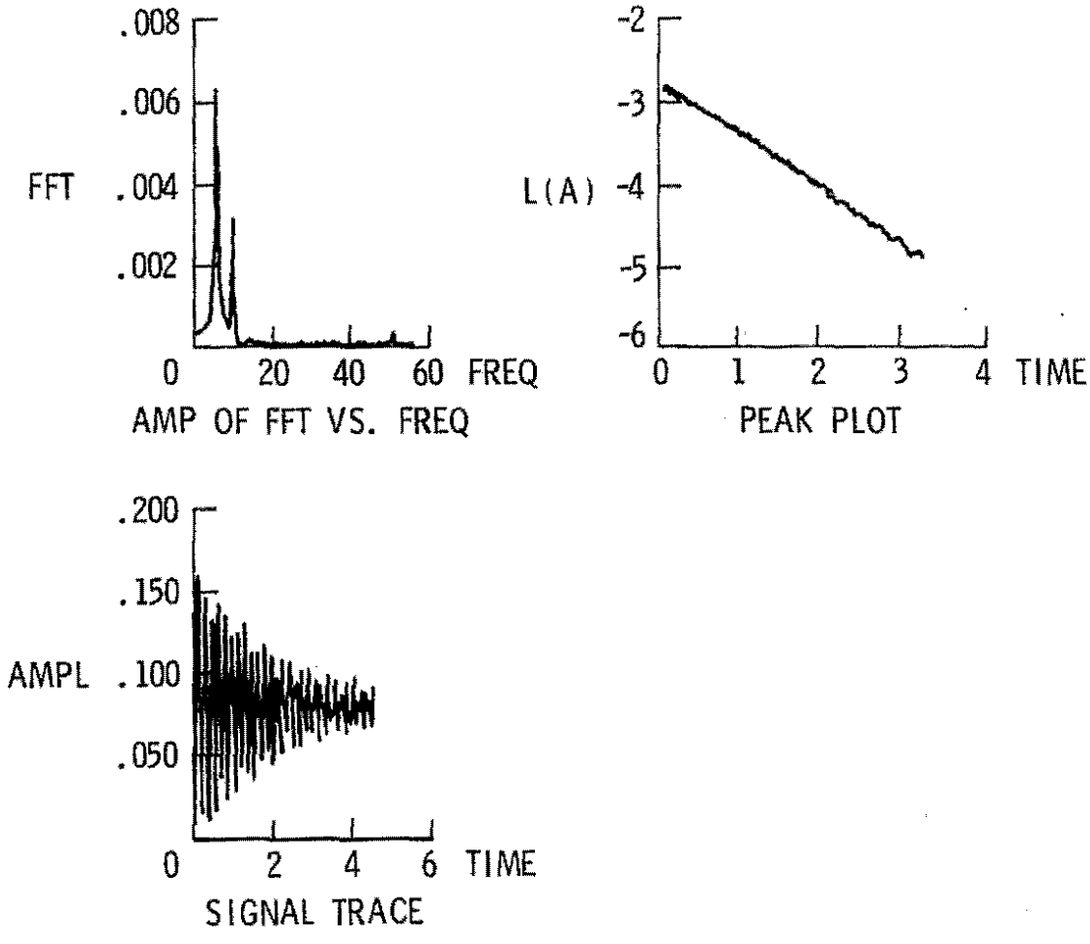

Figure 4. Sample real-time display of moving-block results.

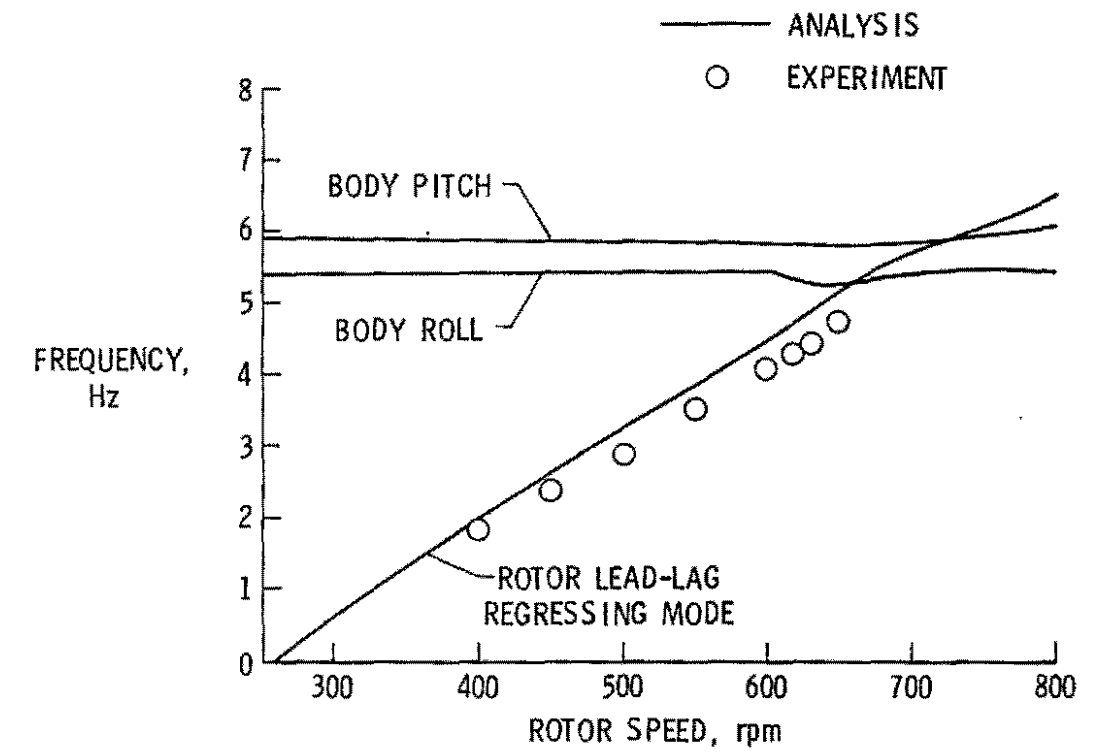

(a) Modal frequencies

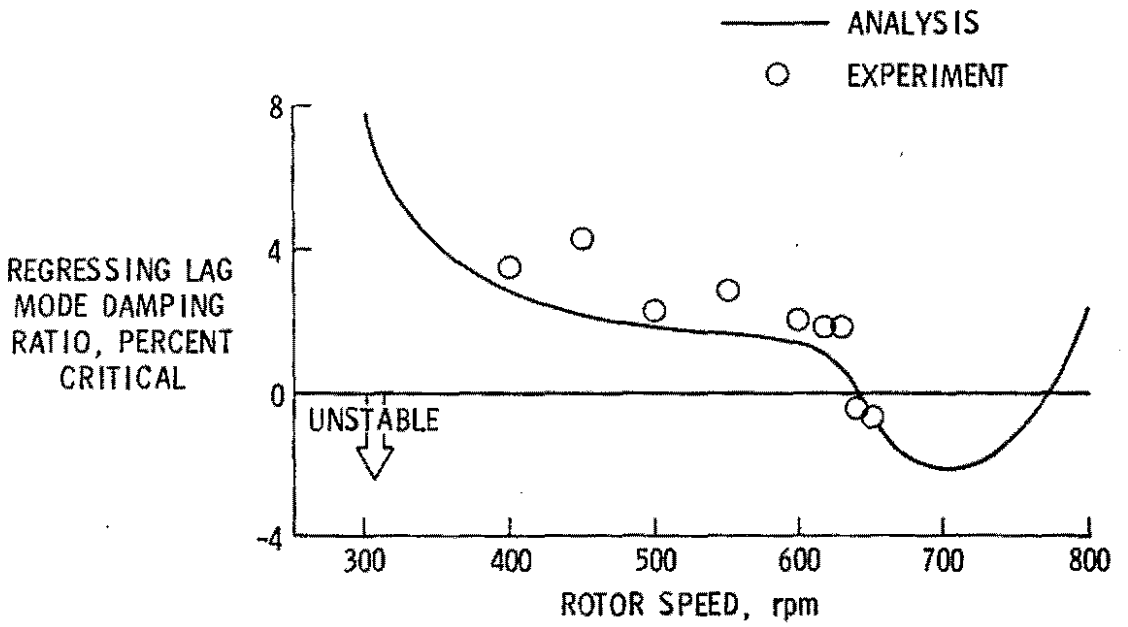

(b) Regressing lag mode damping ratio

Figure 5. Comparison of predicted and measured stability as a function of rotor speed in hover for Configuration 1.

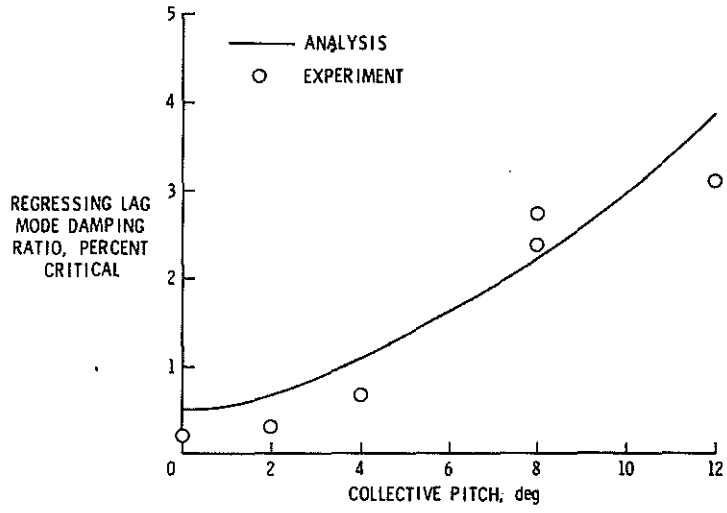

(a) Advance ratio = 0.20

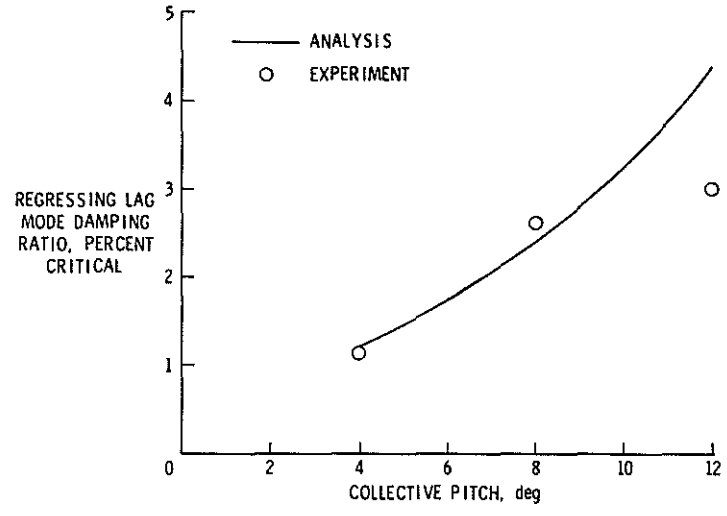

(b) Advance ratio = 0.25

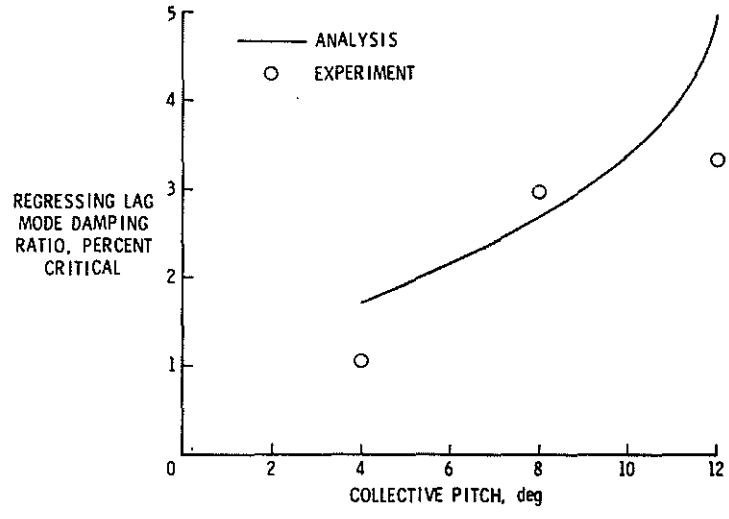

(c) Advance ratio = 0.30

Figure 6. Lead-lag damping as a function of collective pitch in forward flight for baseline configuration.

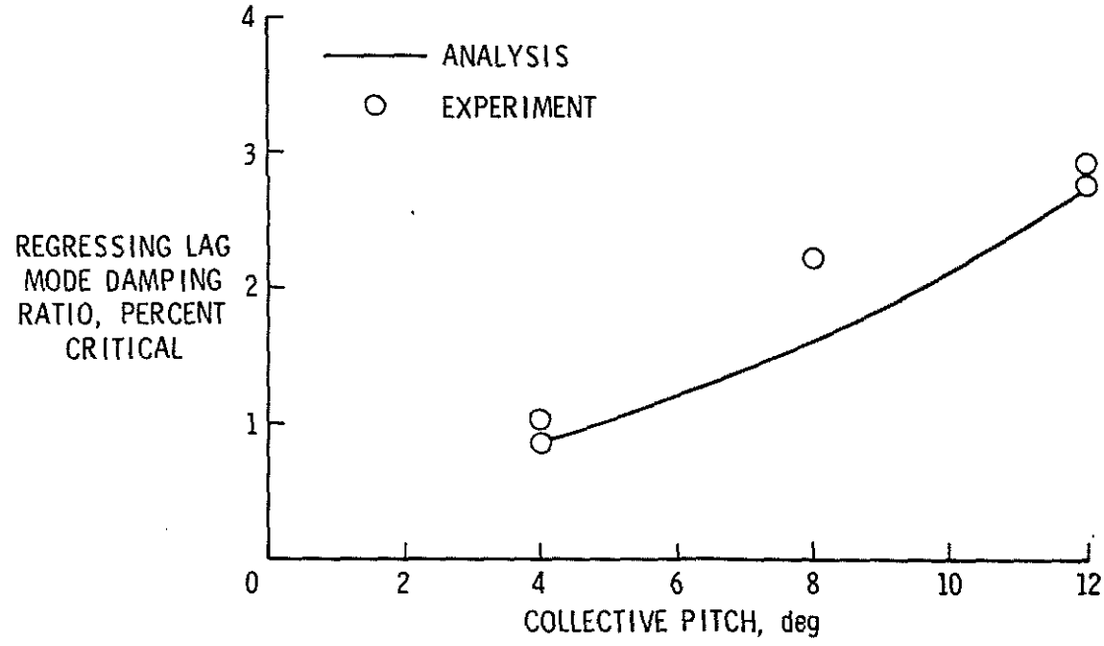

(a) Advance ratio = 0.20

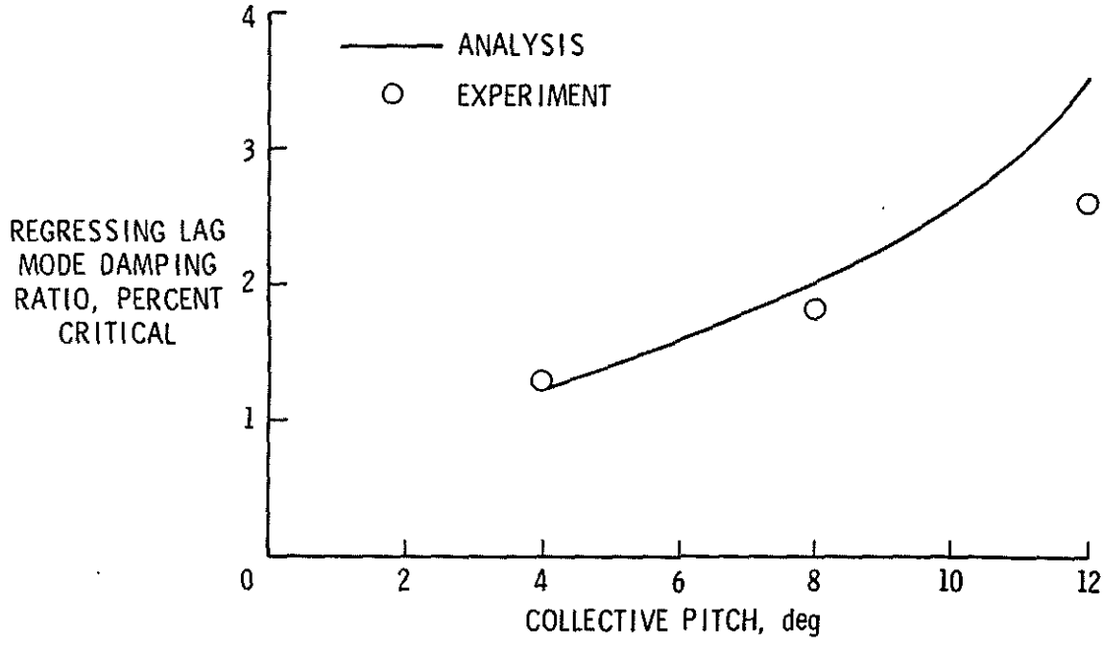

(b) Advance ratio = 0.30

Figure 7. Lead-lag damping as a function of collective pitch in forward flight for Configuration 1.

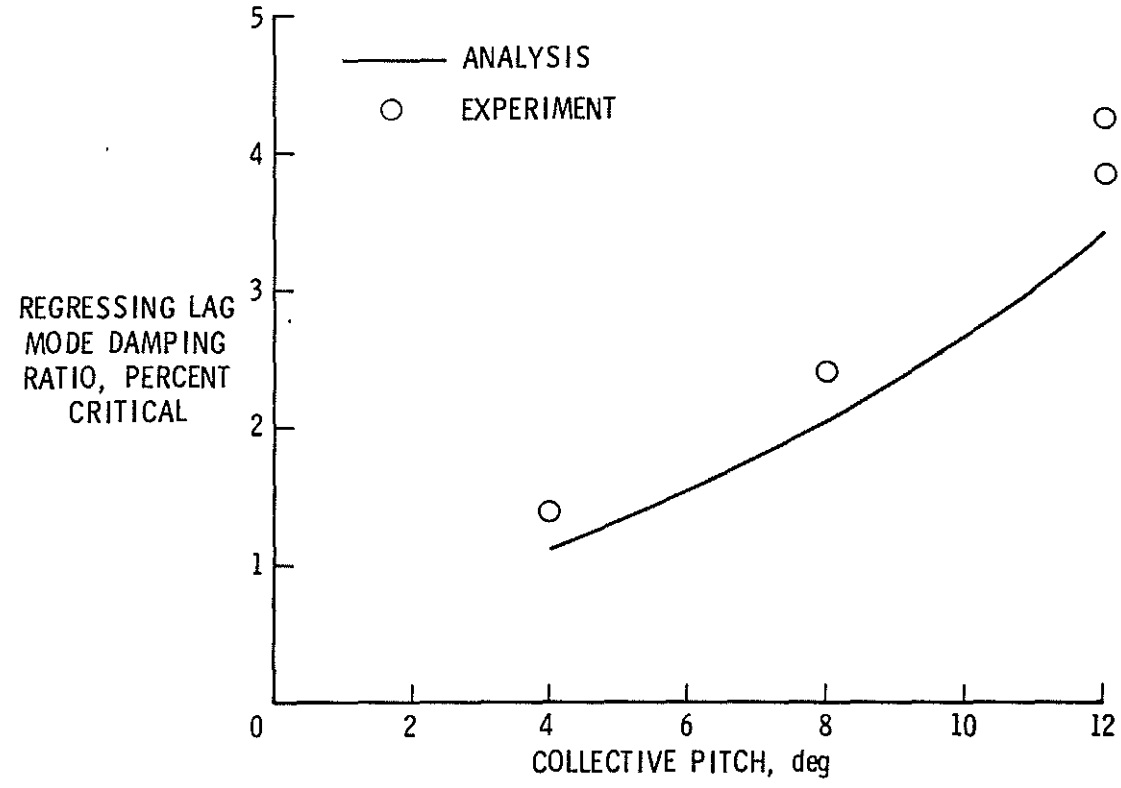

(a) Advance ratio = 0.20

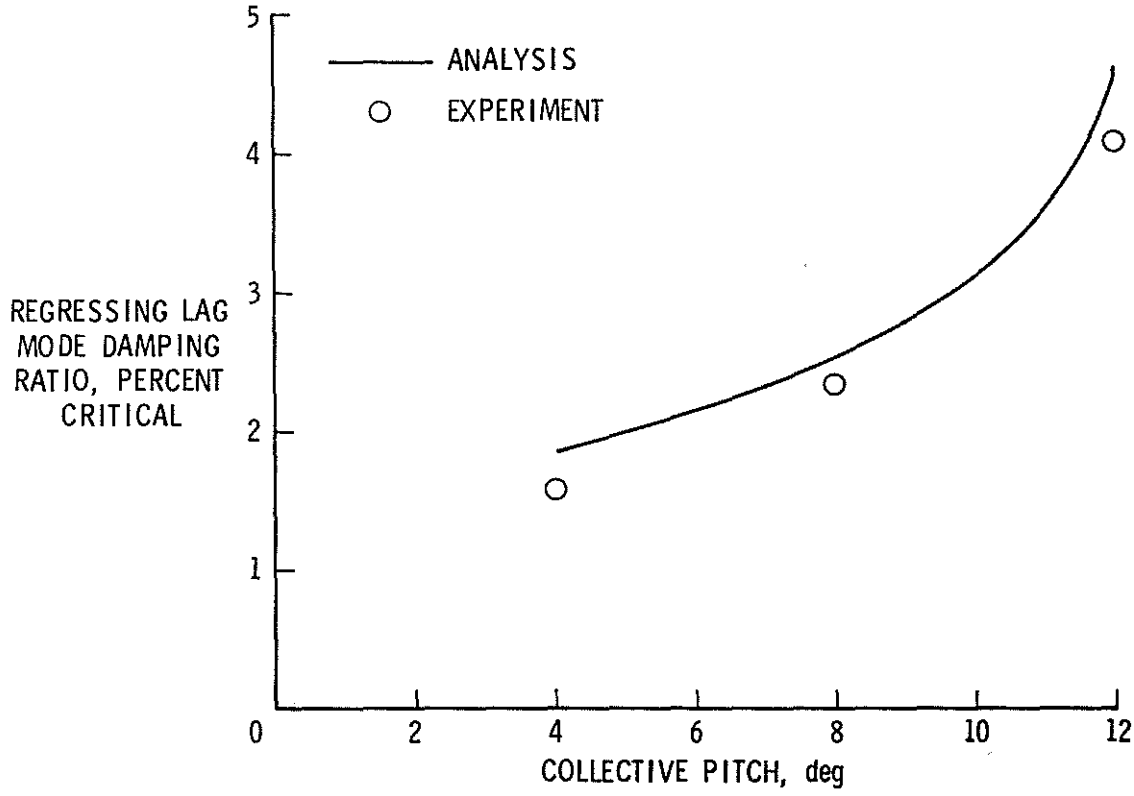

(b) Advance ratio = 0.30

Figure 8. Lead-lag damping as a function of collective pitch in forward flight for Configuration 2.

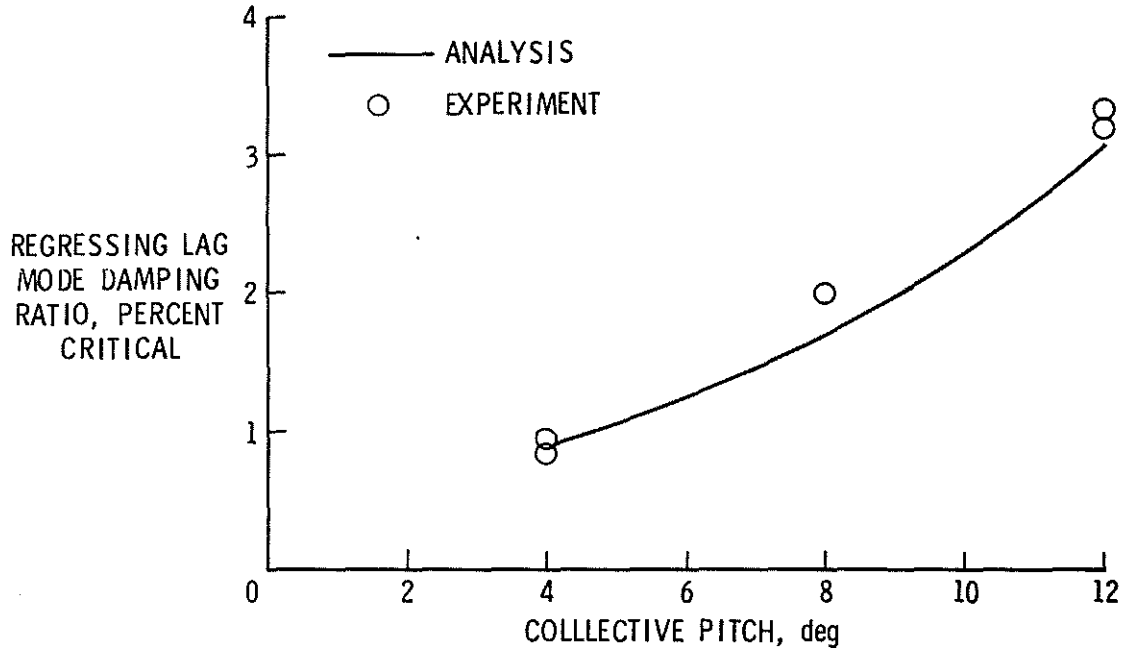

(a) Advance ratio = 0.20

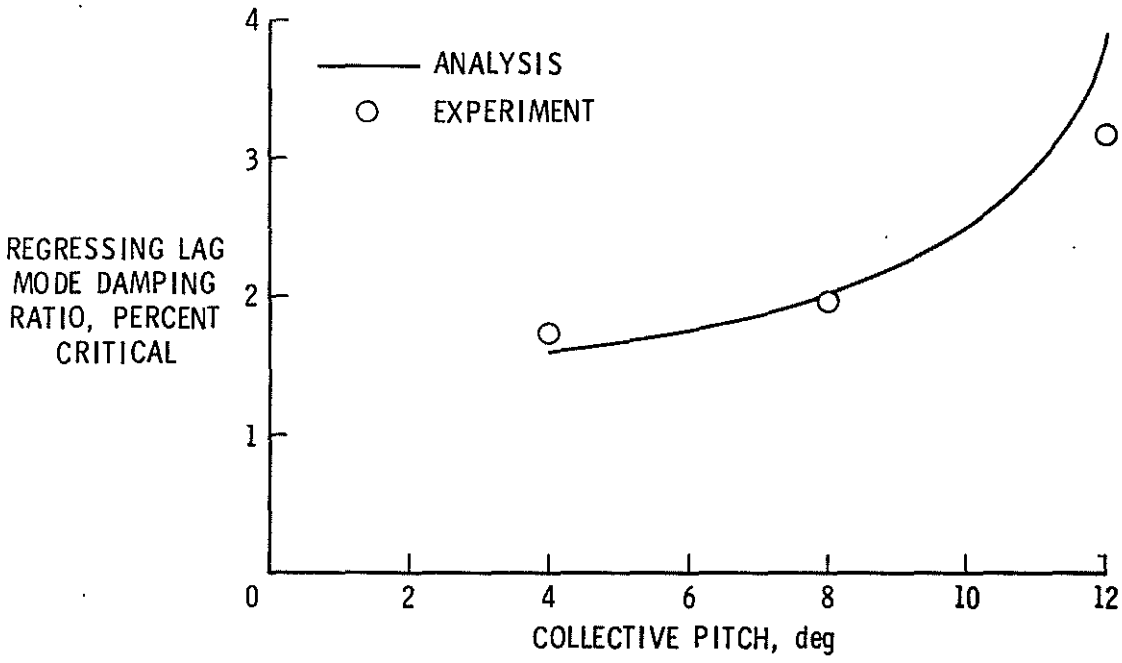

(b) Advance ratio = 0.30

Figure 9. Lead-lag damping as a function of collective pitch in forward flight for Configuration 3.

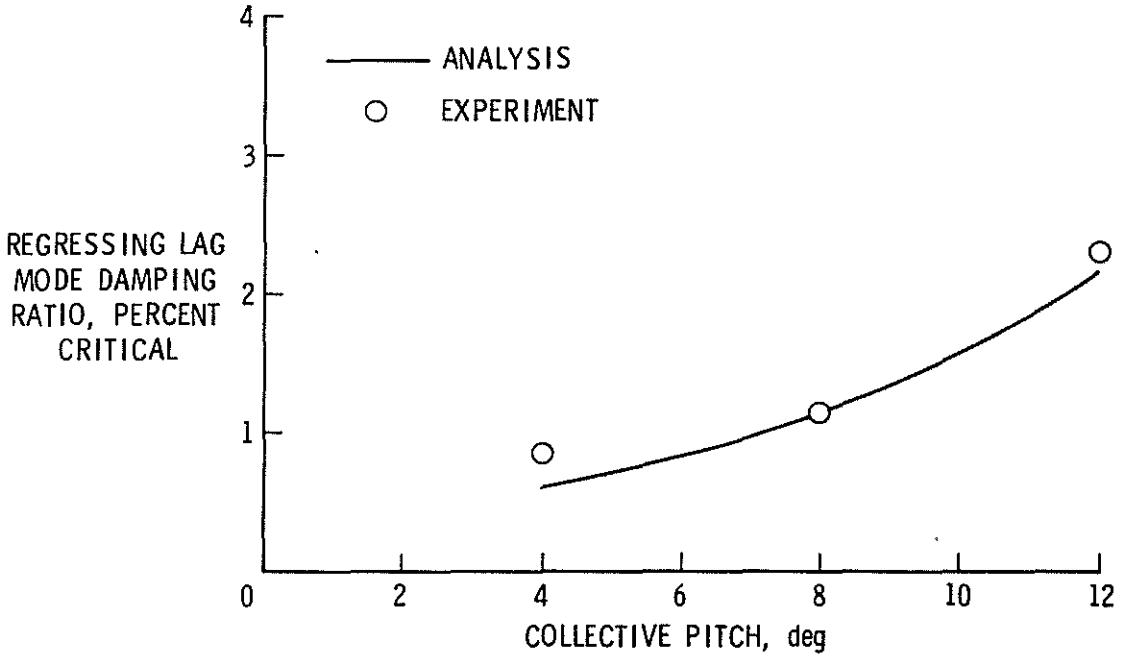

(a) Advance ratio = 0.20

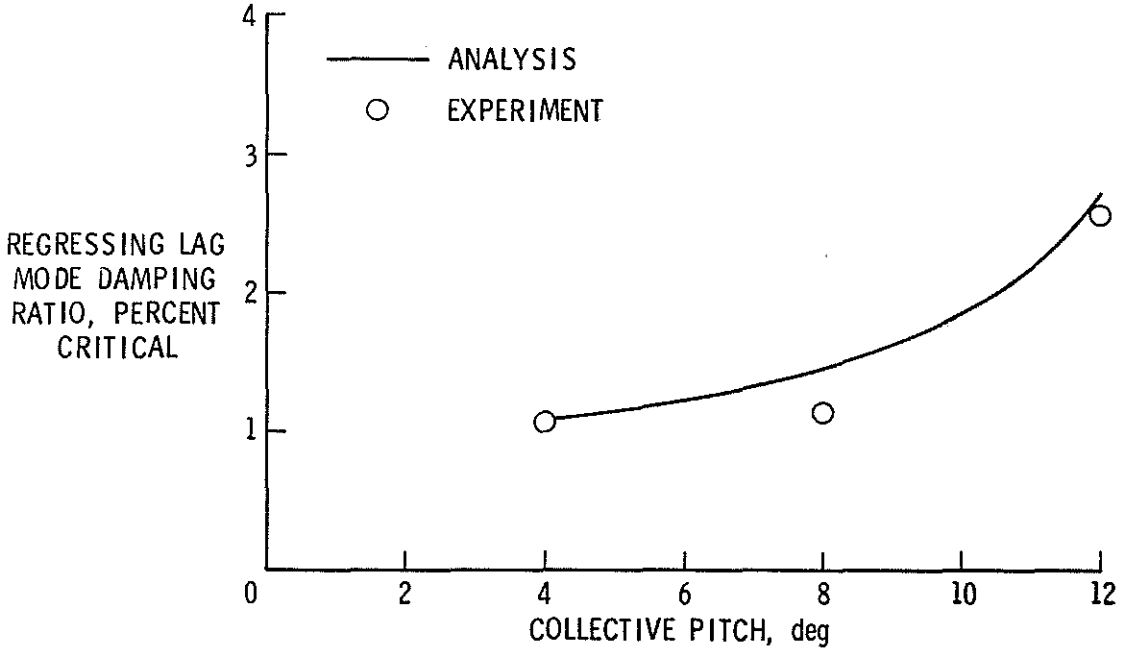

(b) Advance ratio = 0.30

Figure 10. Lead-lag damping as a function of collective pitch in forward flight for Configuration 4.

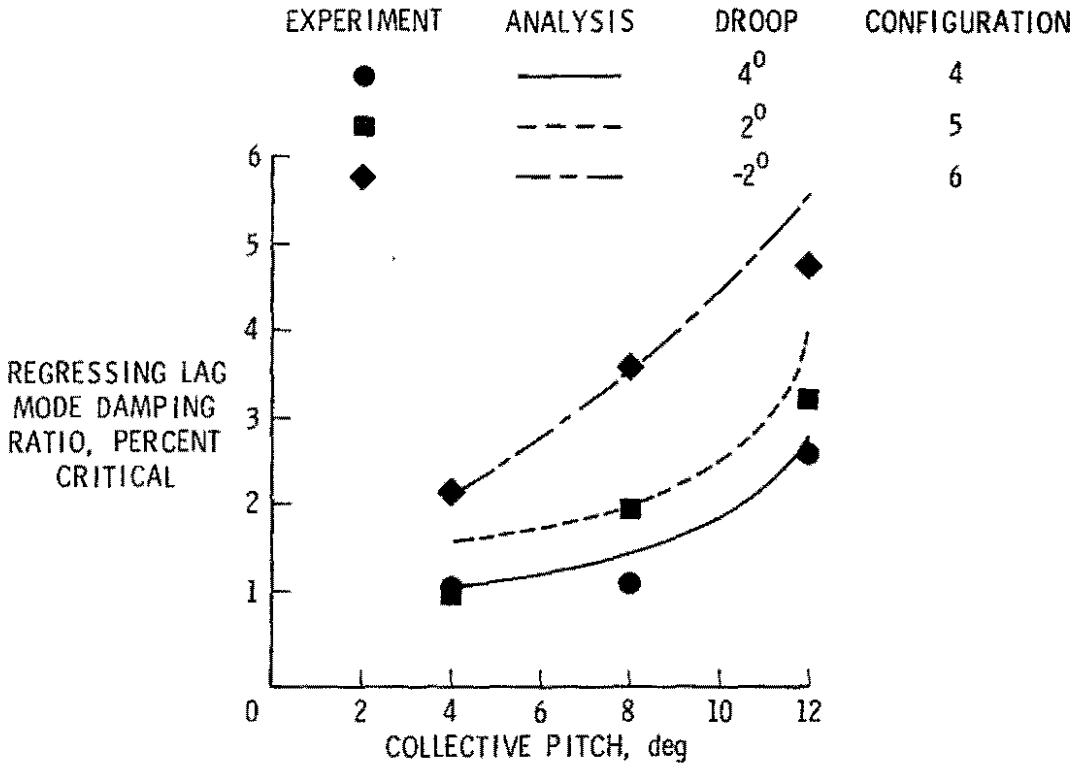

Figure 11. Effect of blade droop angle on lead-lag damping at advance ratio = 0.30.

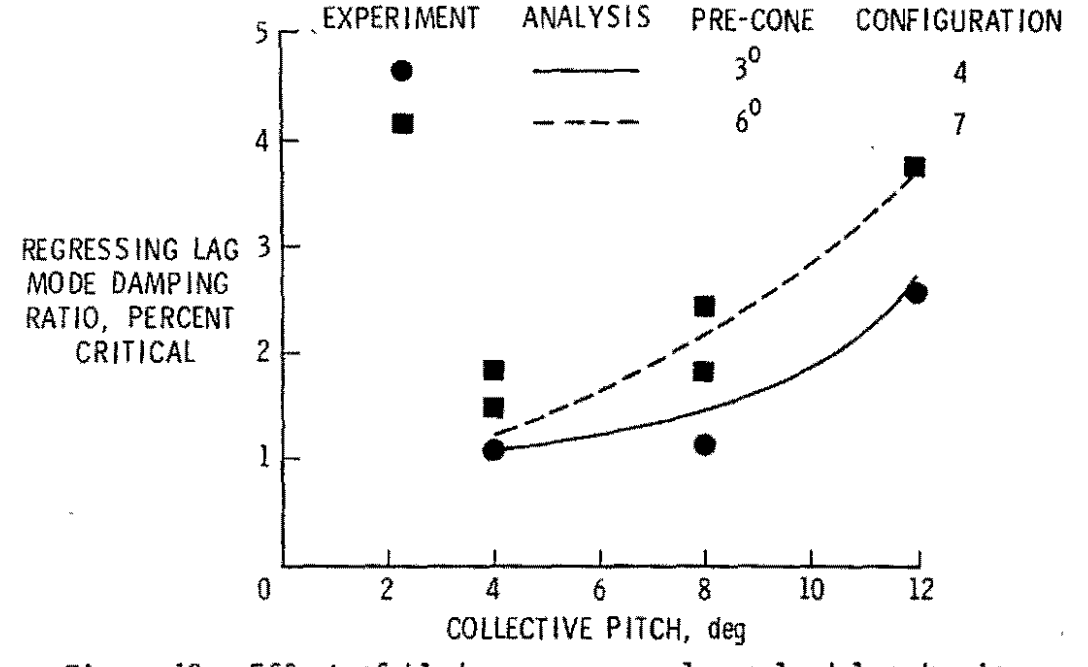

Figure 12. Effect of blade pre-cone angle on lead-lag damping at advance ratio = 0.30.